ELSEVIER

Journal of Power Sources 79 (1999) 97–104

JOURNAL OF POWER SOURCES

Characterization of EP-ash, collected at fossil fuel power plants, as electrode material

S. Ujiie, E. Yagasaki *

Technical Research Center, The Kansai Electric Power Company Inc., 3-11-20, Nakoji, Amagasaki, Hyogo 661-0974, Japan

Received 22 December 1998; accepted 3 January 1999

Abstract

This study deals with the electrochemical properties of fly ash collected by electrostatic precipitators at fossil-fuel power plants. The collected samples, called EP-ash, consist mainly of carbon with a microporous spherical morphology. The EP-ash electrodes show lithium insertion–extraction ability with some irreversible capacity. A simple washing treatment improves the electrochemical properties. The EP-ash can be charged and discharged successfully beyond 100 cycles with a reversible capacity above 200 mA h g^{-1}, even though it contains many contaminants.

Keywords: Electrode; Fly ash; Waste; Lithium-ion battery; Electrostatic precipitator; Carbon

1. Introduction

Lithium-ion batteries are widely used as power sources for portable electrical appliances due to their high voltage and high specific energy. The success of this technology was brought by the usage of carbonaceous material with lithium insertion capability, instead of metallic lithium, for electrodes. With the rapid development of the lithium-ion battery, various carbon materials have been investigated extensively [1,2]. The lithium insertion ability of most of the carbon electrodes is based on the intercalation and de-intercalation properties of the graphite structure. Carbonaceous materials with disordered structure have also collected attention, however, because of their high electrochemical capacities.

Although the novel synthesized carbons show high capacities and other good characteristics as electrode material, they need to undergo an expensive process, viz., heat treatment at temperatures as high as 1000° to 3000°C in an inert atmosphere [3–5]. Cost reduction is essential for lithium-ion battery technology to achieve further extension to large-scale applications such as power sources for electric vehicles and energy-storage systems. There is a search for lower-price materials, not only for positive electrodes, electrolytes or separators, but also for negative electrodes.

On the other hand, recycling of waste has become an important issue more than ever for industries. As a power supplier, the authors' company treats a very large amount of fly ash as waste. It is collected with electrostatic precipitators at oil-fired thermal power plants, and is called EP-ash. In 1995, the amount of the EP-ash exceeded 13 000 ton/year (including water content) at the authors' company [6]. Although it is called 'ash', a large portion of the EP-ash consists of small particles of unburned fuel when the fuel is oil [7]. Therefore, one of the principal components of dried EP-ash is carbon.

This paper is the first demonstration that EP-ash can be used as an electrode material for lithium-ion batteries.

2. Experimental

2.1. Sample preparation

The specimens used in this study were obtained from electrostatic precipitators at some of the fossil-fuel power plants of the authors' company. Samples A1 and A2 were collected from a crude oil combustion boiler, and samples B1 and B2 from a power plant firing heavy oil. The boilers of both power plants were operated at 1200° to 1300°C. Samples A1 and B1 were collected ash powders which had undergone a simple drying treatment at 150°C in atmosphere for 4 days. Samples A2 and B2 were prepared from

* Corresponding author. E-mail: k455792@kepco.co.jp

0378-7753/99/$ - see front matter
PII: S0378-7753(99)00050-6

samples A1 and B1, respectively, by a washing treatment with water as follows: the dried powder A1 or B1 was put in a flask with deionized water of 10 times as much as the sample powder by weight, stirred at room temperature for 2 h, suction-filtered, rinsed with excess deionized water, and dried in air at 150°C for 4 days. Natural graphite (NG-12, The Kansai Coke and Chemicals) was used for comparison measurements. $LiCoO_2$ (Cellseed C-7, Nippon Chemical Industrial) was employed as the cathode material for the test cell using the EP-ash anode.

2.2. Sample characterization

Qualitative and quantitative analyses of the prepared EP-ash samples were made using a vario EL elemental analyzer (Elementar) and a RIX 3000 X-ray fluorescence

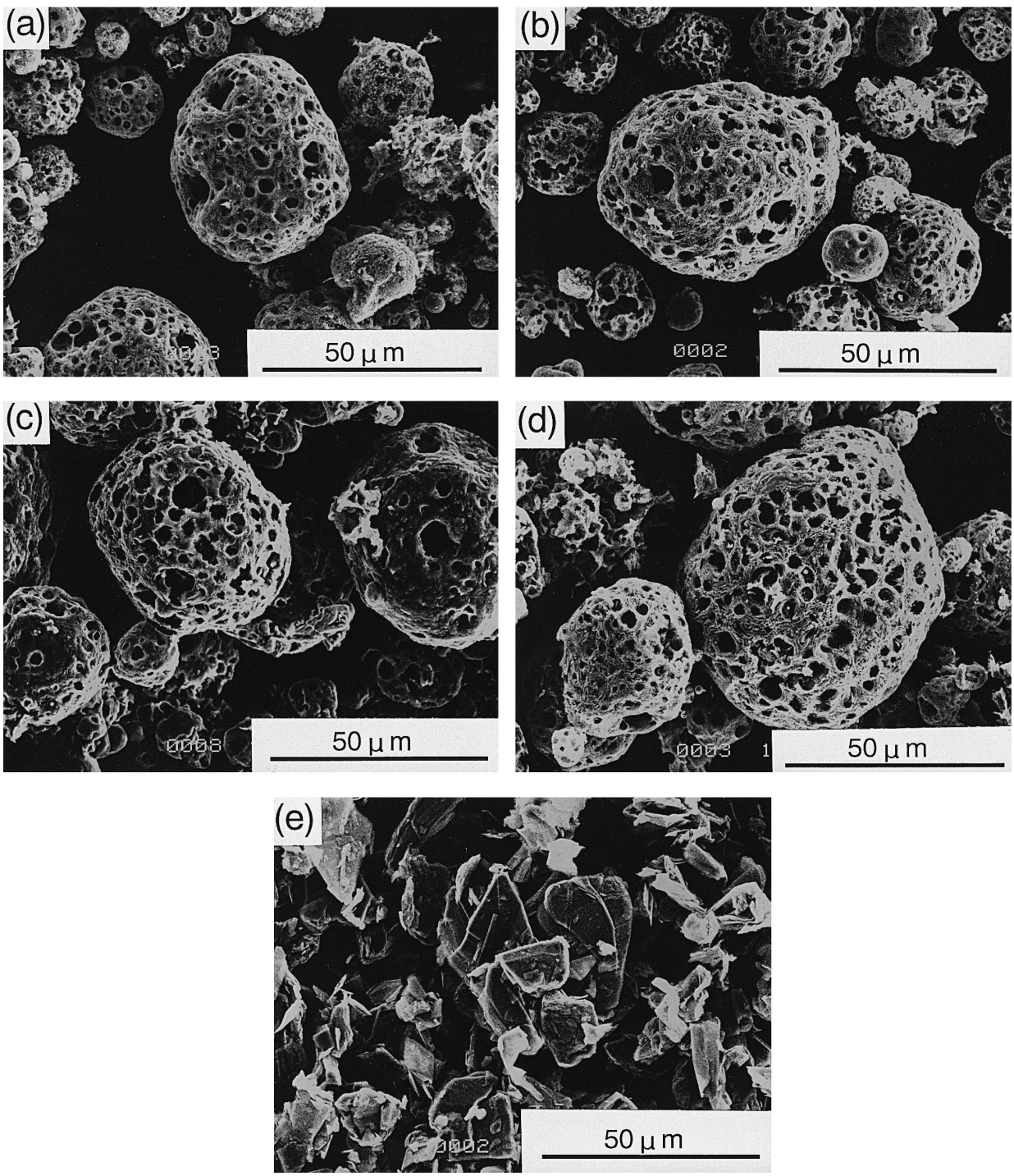

Fig. 1. Electron micrographs of EP-ash samples and natural graphite: (a) sample A1; (b) sample A2; (c) sample B1; (d) sample B2; (e) natural graphite.

Table 1
Analysis results of EP-ash samples

Sample	Quantitative analysis (wt.%)				Semi-quantitative analysis (ppm)						BET surface area ($m^2\ g^{-1}$)
	C	H	N	S	Na	Al	Si	V	Fe	Ni	
A1	89.0	0.5	2.1	1.9	10000	1000	2000	600	6000	8000	18.2
A2	94.2	0.4	1.8	0.7	500	1000	2000	300	6000	5000	34.0
B1	67.5	1.5	5.8	8.1	5000	4000	5000	6000	6000	6000	2.3
B2	91.1	0.2	1.4	3.1	500	5000	9000	5000	6000	5000	13.7

Samples A1 and A2 were obtained from combustion of crude oil; B1 and B2 from heavy oil.
Samples A1 and B1 were prepared through drying, while A2 and B2 underwent drying, washing with deionized water, followed by further drying (See text).
Other detected elements are Mg, P, Cl, K, Ca, Ti, Mn, Co, Cu, Zn, As, Br, Sr, Zr, Mo, Ba and Pb.

analyzer (Rigaku). The sulfur content was examined by titration. The specific area of the samples was measured by means of the Brunauer–Emmett–Teller (BET) method using a BELSORP 36 gas adsorption analyzer (Bel Japan). The filtrates collected from the washing treatment of the EP-ash samples were also analyzed by atomic absorption spectroscopy (AAS) using a Hitachi 180-80 instrument, inductively coupled plasma spectroscopy (ICP) using SPS4000 and SPS1200VR (Seiko instruments) and ion chromatography using DX-500 and DX-120 (Dionex).

The morphology of the samples was observed by means of a scanning electron microscope S-2380N (Hitachi). Powder X-ray diffraction patterns of the EP-ash samples and natural graphite were also measured with an XRD-6000 diffractometer (Shimadzu) with Cu Kα line.

2.3. Electrochemical cell preparation

The electrochemical behaviour of the samples was investigated in three-electrode electrochemical cells. The sheet-type working electrodes were prepared by mixing the EP-ash sample with polytetrafluoroethylene (PTFE) powder (Teflon 62-J, Du pont-Mitsui Fluorochemicals) in a 94:6 ratio by weight in an agate mortar with a pestle, and rolling on an agate board with a PTFE rod. In the case of the natural graphite electrode, 50 wt.% of PTFE was mixed. The sheet was cut into a square piece of dimensions $10 \times 10 \times 0.1$ mm, and pressed on nickel mesh current-collector. Lithium metal (0.1 mm in thickness, Honjo metal) served as the counter and the reference electrodes with nickel mesh current-collectors. The separator was a glass filter (18 mm in diameter, 2 mm in thickness). Test cells were assembled in a glove box filled with argon which had a moisture level kept under 1 ppm. The reference electrode, a separator, the working electrode, a separator and the counter electrode were stacked in order between polypropylene plates. The stack was put into electrolyte in a glass vessel. The electrolyte was 1 M $LiClO_4$ in a 1:1 volume ratio of ethylene carbonate (EC) and diethyl carbonate (DEC) (Sol-Rite, Mitsubishi Chemical). The test cells were o-ring sealed, and removed from the glove box to investigate the electrochemical characteristics.

Some test cells which consisted of the EP-ash working electrode and a counter electrode containing $LiCoO_2$ as active material were also fabricated. The $LiCoO_2$ electrode was prepared from the mixture of $LiCoO_2$ (75 wt.%), PTFE (15 wt.%) and acetylene black (10 wt.%, Denka). The electrodes were prepared in the same manner as described above. A lithium metal electrode was put into the cell to consume the irreversible capacity of the EP-ash electrode before charge–discharge tests of the $LiCoO_2$–EP-ash cell.

2.4. Electrochemical measurements

Charge–discharge characteristics of the test electrodes were investigated by a constant-current method which employed TOSCAT-3100 charge–discharge equipment (Toyo-system). The current was 3.72 or 37.2 mA g^{-1} for

Table 2
Analysis results of filtrate

Washed sample	Dissolved components (ppm for washed sample weight)											
	Na	Fe	Ni	V	Al	Si	Ca	As	P	SO_4^{2-}	Cl^-	NH_4^+
A1	3100	750	3400	190	81	65	470	5.0	4.3	37000	25	5900
B1	1300	2600	2700	1900	180	2.6	430	2.7	16	170000	6.1	57000

Anions and NH_4^+ are quantified with ion chromatography.
Other elements are analyzed with AAS and ICP.

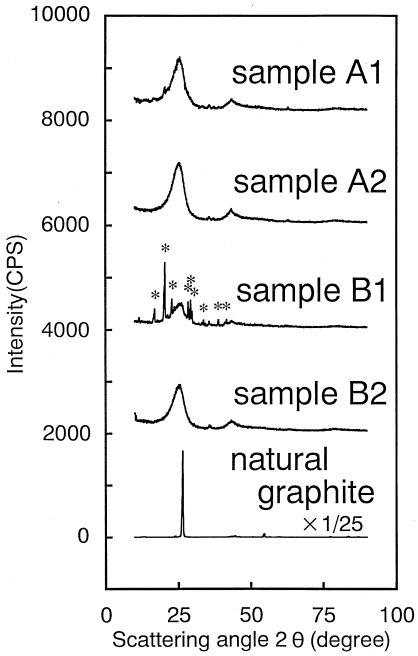

Fig. 2. X-ray diffraction patterns of EP-ash samples and natural graphite. Each pattern is offset vertically by 2000 for clarity. The data for natural graphite are divided by 25. Peaks indicated by * in sample B1 pattern are attributed to $(NH_4)_2SO_4$.

the EP-ash weight, and corresponded to about 0.02 or 0.2 mA cm^{-2} for the electrode, respectively. The cut-off potentials were 0.02 and 1.50 V (vs. Li/Li^+), and the cell was rested for 30 min after each charge or discharge. Cyclic voltammetry was also carried out for some of the EP-ash electrodes using an HZ-A1 system (Hokuto-Denko). The potential of the test electrodes was scanned between 0 and 3.5 V (vs. Li/Li^+) for three cycles at 0.1 mV s^{-1}.

The performance of the cell with an EP-ash negative electrode and a $LiCoO_2$ positive electrode was studied as follows: first, lithium-ions were inserted into the EP-ash electrode at a current of 18.6 mA g^{-1} for the EP-ash weight to a cut-off voltage of 0.02 V vs. Li/Li^+, then extracted at the same current to 1.50 V. The irreversible

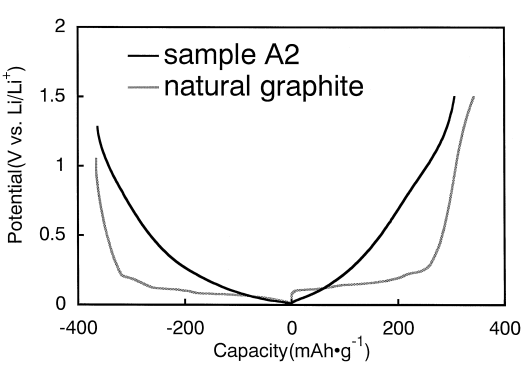

Fig. 3. Potential profiles for electrodes of washed EP-ash sample A2 and natural graphite. Current = 3.72 mA g^{-1} for sample weights and cut-off potentials = 0.02 and 1.50 V (vs. Li/Li^+).

capacity of the EP-ash electrode is consumed with this initial treatment. After this first cycle, charge–discharge measurements using EP-ash and $LiCoO_2$ were carried out with a constant current of 15.6 mA g^{-1} for the $LiCoO_2$ weight. The cut-off voltages were 1.00 and 4.18 V and the cut-off capacity was 125 mA h g^{-1} for $LiCoO_2$.

3. Results

3.1. Characterization of EP-ash

Scanning electron micrographs of the samples are shown in Fig. 1. All EP-ash powders have spherical shapes of 5 to 50 μm in diameter (Fig. 1a–d). The particles have very

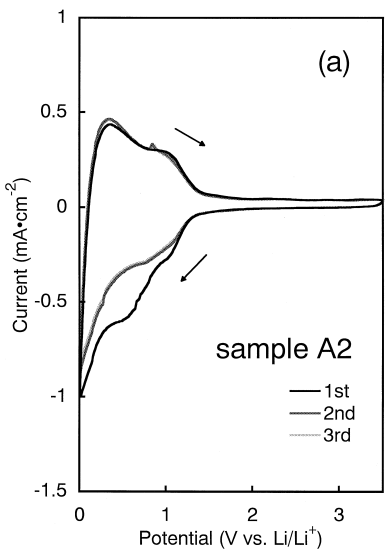

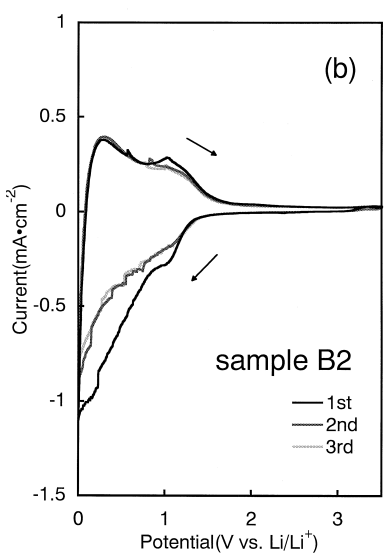

Fig. 4. Cyclic voltammograms for EP-ash electrodes: (a) sample A2; (b) sample B2. Scan rate = 0.1 mV s^{-1} and potential is swept between 0 and 3.5 V (vs. Li/Li^+) for three cycles. Direction of potential sweep indicated by arrows.

porous and wrinkly morphologies. By contrast, the natural graphite sample has a flake structure. Some fragments of material are observed on the surface of the dried ash sample B1 particles, but disappear on the washed ash sample B2.

The analysis results of the EP-ash samples are listed in Table 1. The EP-ash samples consist mainly of carbon; in the samples A1 and B1, the carbon contents are 89.0 and 67.5 wt.%, respectively. The carbon content increases to 94.2 wt.% in sample A2 and 91.1 wt.% in sample B2 due to the washing treatment, while there is a decrease in the contents of hydrogen, nitrogen, sulfur and sodium. The BET surface area of sample A1 and B1 is 18.2 and 2.3 $m^2 g^{-1}$, respectively, and increases after the washing treatment.

Table 2 shows the analysis results of the filtrates collected during the washing treatment of the EP-ash samples. The main dissolved components of the filtrates are SO_4^{2-} and NH_4^+.

The XRD patterns of the EP-ash samples and the natural graphite are given in Fig. 2. For natural graphite, a strong sharp peak appears at 26.4°, as expected, and indicates a good crystallinity of the graphitic structure [8]. On the other hand, the (002) peak of the EP-ash samples is weaker and broader. The (002) peaks are observed at lower angles than that of the natural graphite. One of the dried ash samples, viz., B1, has lots of extra peaks but they disappear in the washed sample, B2. The extra peaks are attributed to $(NH_4)_2SO_4$ [9].

3.2. Electrochemical studies

The potential profiles of the sample A2 electrode and the natural graphite electrode at a constant current of 3.72 mA g^{-1} are shown in Fig. 3. The potential of the sample A2 electrode changes continuously, while that of the natural graphite electrode has a flat shape. Nevertheless, the capacity of sample A2 is similar to that of natural graphite. The electrochemical capacity of lithium insertion and extraction into/from sample A2 is 363 and 307 mA h g^{-1}, respectively, at the rate of 3.72 mA g^{-1} in the potential range 0.02 to 1.50 V (vs. Li/Li^+).

Cyclic voltammograms for the EP-ash electrodes are given in Fig. 4. The samples A2 and B2 display almost the same profile. A redox current is obtained between 0 and 1.5 V (vs. Li/Li^+). The current of the first reduction is larger than that of the second cycle, while the profile of the third cycle is almost the same as that of the second cycle. The oxidation current profiles of the first, second and third cycles are similar with a broad peak at 0.3 V (vs. Li/Li^+), in spite of few small spikes.

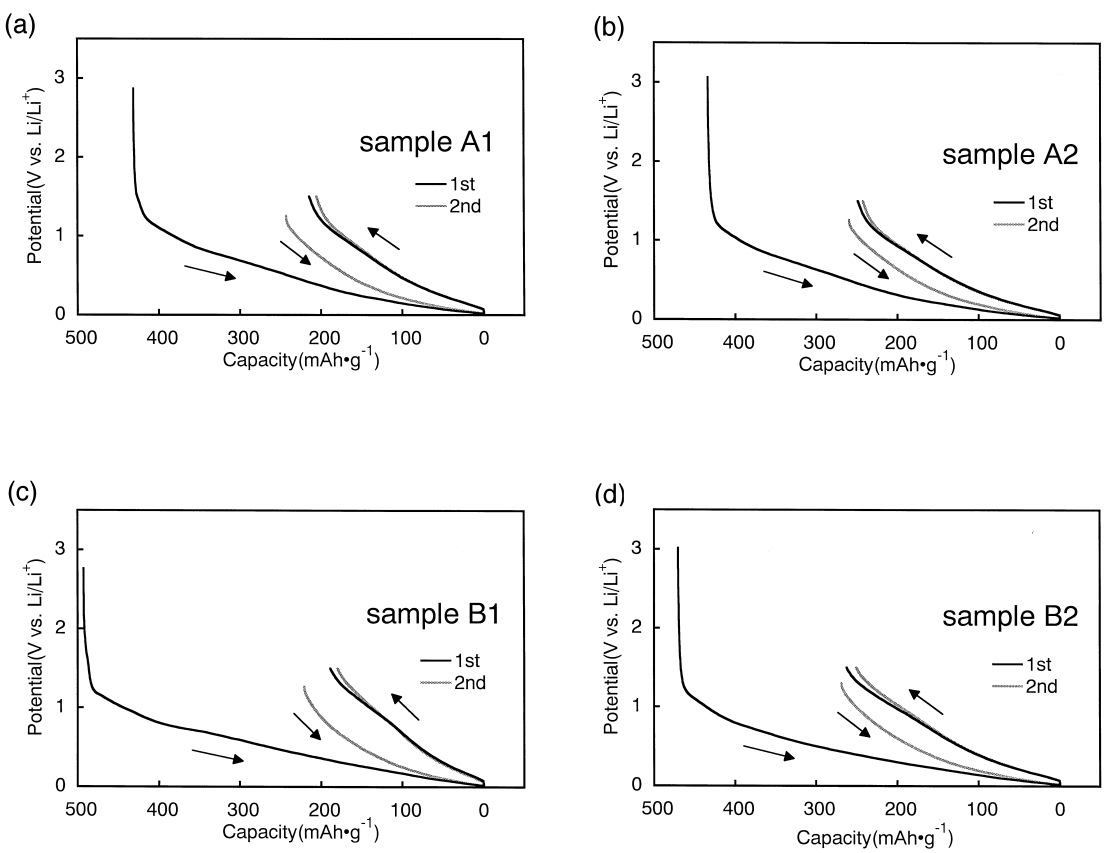

Fig. 5. Potential profiles for EP-ash electrodes on first and second cycle: (a) sample A1; (b) sample A2; (c) sample B1; (d) sample B2. Current = 37.2 mA g^{-1} for sample weights and cut-off potentials = 0.02 and 1.50 V (vs. Li/Li^+). Direction of charge and discharge indicated by arrows.

The charge–discharge properties of the EP-ash electrodes were investigated at a constant current of 37.2 mA g^{-1}. The potential profiles of the EP-ash electrodes during the first and second cycles are presented in Fig. 5. The potential of each cycle changes continuously. A large irreversible capacity is observed on the first cycle for all samples. The irreversible capacity of the dried ash samples A1 and B1 is 217 and 305 mA h g^{-1}, respectively, but are smaller when washed ashes are used viz., 185 and 208 mA h g^{-1} for samples A2 and B2, respectively. The washing treatment also improves the electrochemical capacity of the first lithium extraction from 214 mA h g^{-1} (dried sample A1) to 249 mA h g^{-1} (washed sample A2) and from 189 mA h g^{-1} (dried sample B1) to 262 mA h g^{-1} (washed sample B2). On the second cycle, the irreversible capacities become much smaller compared with those for the first cycle. The reversible capacities of the second cycle are around 200 mA h g^{-1} for all the EP-ash samples.

The cycling performance of the ash samples is shown in Fig. 6. In the case of the washed ash samples A2 and B2, the capacities decrease gradually from the 1st to 20th cycle, then stay almost constant. The capacities are more than 200 mA h g^{-1} beyond 100 cycles; the capacities of the lithium-ion insertion and extraction at the 100th cycle are 218 and 217 mA h g^{-1} for sample A2, and 205 and 204 mA h g^{-1} for sample B2, respectively. The coulombic efficiencies are 99.7% (sample A2) and 99.6% (sample B2). On the other hand, the capacities of the dried ash samples A1 and B1 deteriorate faster than those of the washed samples.

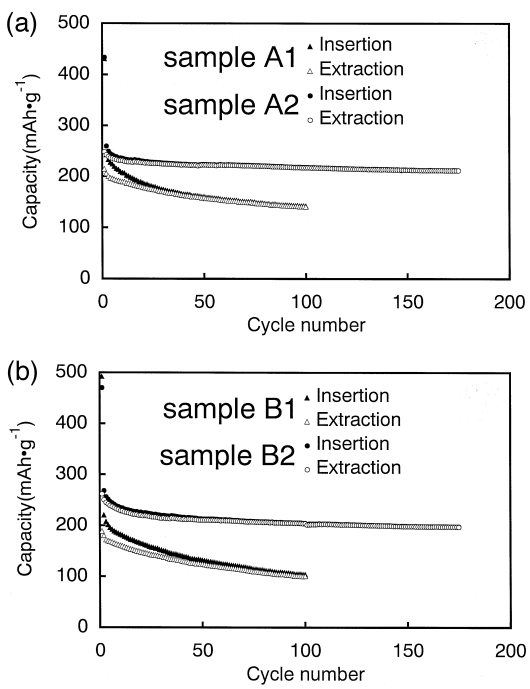

Fig. 6. Cycling performance of EP-ash electrodes: (a) samples A1 and A2; (b) samples B1 and B2. Current = 37.2 mA g^{-1} for sample weights and cut-off potentials = 0.02 and 1.50 V (vs. Li/Li^+).

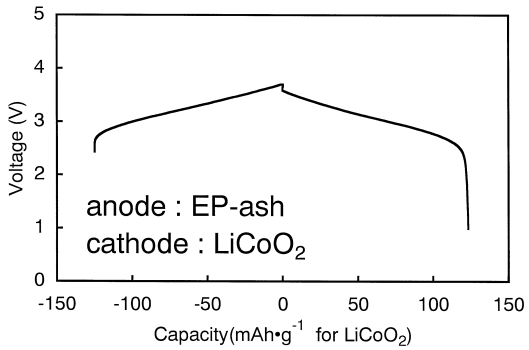

Fig. 7. Charge and discharge profile for a cell with an EP-ash negative electrode and $LiCoO_2$ positive electrode. Weight ratio of EP-ash and $LiCoO_2$ = 100:75. Current = 15.6 mA g^{-1} for $LiCoO_2$. Cut-off voltages = 1.00 and 4.18 V. Cut-off capacity = 125 mA h g^{-1} for $LiCoO_2$.

The performance of the EP-ash as a negative-electrode was also examined in a lithium-ion battery. The voltage profile of a cell which has sample A2 as the negative electrode and $LiCoO_2$ as the positive electrode is shown in Fig. 7. The irreversible capacity of the EP-ash electrode was consumed with an extra lithium electrode before the EP-ash/$LiCoO_2$ cell was tested. The cell can be charged and discharged around 3.2 V with a very smooth voltage profile. In this experiment, charging is cut by a capacity trigger and discharging is finished by a voltage trigger. The coulombic and energetic efficiencies are 98.7 and 92.4%, respectively.

4. Discussion

4.1. Characterization of EP-ash

Carbon is the main component of all the EP-ash samples, as shown in Table 1. The carbon concentration varies with the origin of the ash and with the treatment which the samples have undergone. Sample A1 obtained from a crude oil combustion has a larger carbon content than sample B1 collected at a heavy oil firing plant. The difference in the carbon content originates from the composition of the fuel used in each power plant as well as the treatment carried out before the sample was collected from the electrostatic precipitator.

As shown in Fig. 1, the morphologies of all the samples look almost the same, independent of the fired oil. The observation also reveals that the EP-ash particles are not destroyed during the washing treatment in spite of their porous structure.

In XRD patterns, the peaks of the EP-ash samples are weak and broad, with the (002) peaks at lower angle compared with the pattern of the natural graphite. This suggests that the carbon of the EP-ash has a graphite structure with a low degree of crystallinity [10].

It is found that the washing treatment certainly improves the properties of the EP-ash as an electrode mate-

rial. The washing treatment causes the carbon concentrations of the samples to increase, and indicates that a large portion of the contaminants in the EP-ash are water-soluble. One of the water-soluble contaminants, $(NH_4)_2SO_4$, is observed in the XRD patterns. The XRD peaks of $(NH_4)_2SO_4$ in the dried sample B1 disappear in the washed sample B2. This is in agreement with the analysis results of the filtrates, as listed in Table 2. At the power plants, ammonia gas is injected into flue gas prior to the electrostatic precipitation to condition the acidity and the electrical resistivity of the fly ash [11]. This procedure results in the formation of $(NH_4)_2SO_4$. Therefore, contamination of the EP-ash by $(NH_4)_2SO_4$ cannot be avoided, but the contaminant is removed easily by the washing treatment. Water-soluble fragments of material are also observed in the SEM image, as shown in Fig. 1c. The fragments on the surface of the sample B1 particles are removed by the washing treatment and porous morphologies appear clearly in the sample B2. Although it is not clear whether the surface fragments are $(NH_4)_2SO_4$ or not, it appears that the increase of the specific area of sample B2 is caused by their removal.

4.2. Electrochemical studies

As shown in Figs. 3 and 5, the potential during charge and discharge of the EP-ash changes continuously. This behaviour is the same as that exhibited by other carbonaceous materials with low crystallinity of the graphite structure [10], and is verified by the above XRD results for the samples.

The washed EP-ash sample A2 yields a large capacity near the theoretical value of 372 mA h g^{-1} for graphite [1] at the constant current of 3.72 mA g^{-1}. Furthermore, the washed EP-ash samples have an excellent reversibility of lithium-ion insertion and extraction as observed in the cyclic voltammetry measurements shown in Fig. 4. These results indicate that the EP-ash is a good material for a lithium-ion insertion electrode despite its low crystallinity.

A large irreversible capacity is observed, however, on the first cycle as shown in Fig. 5. It also appears as a large reduction current on the first cycle in the cyclic voltammogram. A large irreversible capacity on the first cycle is often observed with disordered carbons [10,12], and indicates that the EP-ash shows the typical behaviour of a disordered carbon during the initial lithium insertion–extraction.

The results reported here show that the irreversible capacity is decreased as the surface area is increased by the washing treatment. It is reported that the irreversible capacity is caused by decomposition of electrolyte on the carbon surface, and is thus proportional to the initial surface area of the carbon [13]. The difference between the EP-ash samples and most of the reported carbon materials is the content of the contaminants. The EP-ash contains a number of elements and ions. Although some of them are removed by washing with water, the EP-ash is still a 'dirty' material compared with most carbonaceous materials which normally contain only trace levels of contaminants. In the EP-ash material, the water-soluble contaminants certainly cause part of the observed irreversible capacity. Their removal not only reduces the electrochemical capacity consumed by side reactions but also increases the surface area of clean carbon where the insertion–extraction of lithium-ions occurs.

Though the irreversible capacity on the first cycle is large, the EP-ash has a reversible capacity of around 200 mA h g^{-1} at a current of 37.2 mA g^{-1}, as shown in Figs. 5 and 6. The lithium insertion and extraction proceed reversibly after the second cycle. The washing treatment also influences the reversible capacity to some degree. First, the washed samples A2 and B2 have larger reversible capacities than the dried samples A1 and B1. It appears that the higher carbon concentrations of the washed samples render the capacities larger. This suggests that the effective surface area for the lithium insertion–extraction is increased by the washing treatment. Second, the washed samples display better cycling performance than the dried ones. The capacities of the washed samples stay almost constant after the 20th cycle, but those of the dried ash samples deteriorate with cycling.

As mentioned above, it is clear that a simple washing treatment reduces the irreversible capacity, increases the reversible capacity, and enhances the cycling ability. These improvements are caused by increase in carbon content, enlargement of the surface area, and decrease of parasitic side reactions involving contaminants.

The most important outcome of this study is the fact that the EP-ash shows good characteristics as a material for lithium insertion electrodes even though it contains many contaminants. Many types of contaminants still remain in the EP-ash samples after the washing treatment, as shown in Table 1, yet electrodes A2 and B2 can cycle more than 100 times without deterioration. The results indicate that a simple washing treatment with water is sufficient to obtain an electrode material with lithium-ion insertion–extraction abilities.

It has also been shown that the EP-ash electrode performs well with the most popular positive electrode, $LiCoO_2$, for commercial lithium-ion batteries. A test battery has a smooth potential profile of around 3.2 V. This suggests that the EP-ash could be a candidate, low-cost material for lithium-ion batteries and, therefore, a promising substitute for expensive synthetic carbons. Application in lithium-ion batteries might be an effective way to reutilize the EP-ash which, at present, is disposed as waste.

5. Conclusions

EP-ash has been studied as a lithium insertion material. The characteristics of the samples are almost the same in

spite of the difference in the origin of the fuel oil. The EP-ash consists mainly of carbon with microporous spherical morphologies. It has a graphite structure with a low degree of crystallinity. Although the EP-ash contains many contaminants, the properties as a lithium insertion material are improved by a simple washing treatment. At a current of 3.72 mA g^{-1}, the washed EP-ash shows a large reversible capacity of lithium insertion–extraction near the theoretical value of 372 mA h g^{-1} for graphite. At a current of 37.2 mA g^{-1}, the reversible capacity is over 200 mA h g^{-1} beyond 100 cycles. The EP-ash electrode performs well with a $LiCoO_2$ positive electrode in a test battery which has a smooth potential profile of around 3.2 V.

The results suggest that EP-ash, now disposed as waste, could be a candidate low-cost material for lithium-ion batteries.

Acknowledgements

The authors are grateful to Dr. Katsumi Yoshino for his useful advice.

References

[1] J.R. Dahn, A.K. Sleigh, H. Shi, B.M. Way, W.J. Weydanz, J.N. Reimers, Q. Zhong, U. von Sacken, in: G. Pistoia (Ed.), Lithium Batteries, New Materials, Developments and Perspectives, Elsevier, Amsterdam, 1994, pp. 1, and references therein.
[2] K. Sawai, Y. Iwakoshi, T. Ohzuku, Solid State Ionics 69 (1994) 273.
[3] A. Mabuchi, K. Tokumitsu, H. Fujimoto, T. Kasuh, J. Electrochem. Soc. 142 (1995) 1041.
[4] N. Takami, A. Satoh, M. Hara, T. Ohsaki, J. Electrochem. Soc. 142 (1995) 2564.
[5] K. Zaghib, K. Tatsumi, H. Abe, T. Ohsaki, Y. Sawada, H. Higuchi, J. Electrochem. Soc. 145 (1998) 210.
[6] A. Baba, T. Yatani, T. Azumi, K. Yamada, Proc. First Intnl. Symp. Incineration and Fuel Gas Treatment Technologies, Combustion Session 3, Abstract No. 2, 1997.
[7] W.M. Henry, K.T. Knapp, Environ. Sci. Technol. 14 (1980) 450.
[8] JCPDS, PDF No. 41-1487, 1996.
[9] JCPDS, PDF No. 40-0660, 1996.
[10] J.R. Dahn, A.K. Sleigh, H. Shi, J.N. Reimers, Q. Zhong, B.M. Way, Electrochim. Acta 38 (1993) 1179.
[11] E.B. Dismukes, Proc. 76th Ann. Mtg. Air Pollution Control Association, Vol. 76 (3), 1983, 831741.3.1.
[12] N. Takami, A. Satoh, T. Ohsaki, M. Kanda, Electrochim. Acta 42 (1997) 2537.
[13] R. Fong, U. von Sacken, J.R. Dahn, J. Electrochem. Soc. 137 (1990) 2009.